Development of a novel antibody-tetrazine conjugate for bioorthogonal pretargeting

Reference:

Maggi Agnese, Ruivo Eduardo, Fissers Jens, Vangestel Christel, Chatterjee Sneha, Joossens Jurgen, Sobott Frank, Staelens Steven, Stroobants Sigrid, van der Veken Pieter, ...- Development of a novel antibody-tetrazine conjugate for bioorthogonal pretargeting

Organic and biomolecular chemistry / Chemical Society [Londen] - ISSN 1477-0520 - 14:31(2016), p. 7544-7551

Full text (Publisher's DOI): http://dx.doi.org/doi:10.1039/C6OB01411A

To cite this reference: http://hdl.handle.net/10067/1357570151162165141

Organic & Biomolecular Chemistry

Accepted Manuscript

This article can be cited before page numbers have been issued, to do this please use: A. Maggi, E. Ruivo, J. Fissers, C. Vangestel, S. Chatterjee, J. Joossens, F. Sobott, S. Staelens, S. Stroobants, P. Van der Veken, L. wyffels and K. Augustyns, *Org. Biomol. Chem.*, 2016, DOI: 10.1039/C6OB01411A.

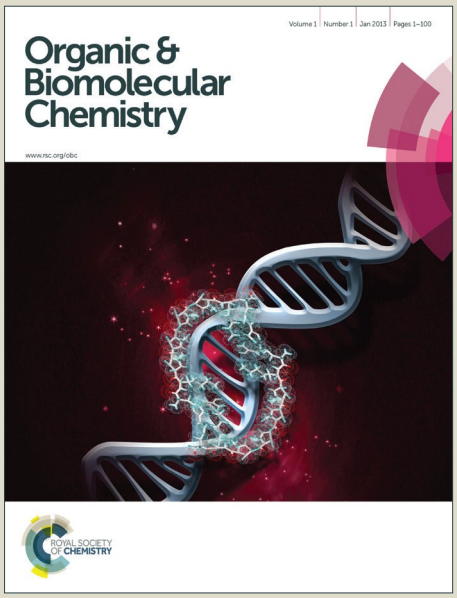

ROYAL SOCIETY OF CHEMISTRY

www.rsc.org/obc

View Article Online
DOI: 10.1039/C6OB01411A

Organic & Biomolecular Chemistry

ARTICLE

DEVELOPMENT OF A NOVEL ANTIBODY-TETRAZINE CONJUGATE FOR BIOORTHOGONAL PRETARGETING

Received 00th January 20xx,
Accepted 00th January 20xx

DOI: 10.1039/x0xx00000x

www.rsc.org/

Agnese Maggi,[a] Eduardo Ruivo,[a] Jens Fissers,[a] Christel Vangestel,[b] Sneha Chatterjee,[c] Jurgen Joossens,[a] Frank Sobott,[c] Steven Staelens,[b] Sigrid Stroobants,[b,d] Pieter Van der Veken,[a] Leonie wyffels,[b,d] Koen Augustyns,[a]†

Abstract. Recently, bioorthogonal chemistry based on the Inverse Electron-Demand Diels-Alder (IEDDA) cycloaddition between 1,2,4,5-tetrazines and trans-cyclooctene (TCO) analogues added an interesting dimension to molecular imaging. Until now, antibodies (Abs) were tagged with TCO and after pretargeting were reacted with tetrazines substituted with reporters. However, TCO tags have the tendency to degrade under physiological conditions, and due to their hydrophobic nature bury within the protein. This results in loss of reactivity and a low Ab functional loading. To circumvent these problems, we report for the first time an approach in which tetrazines are used as tags for antibody (Ab) modification, and TCO as imaging agent. We developed a new Ab-tetrazine conjugate which displays high functional loading, good stability and reactivity. We utilized this immunoconjugate for live-cell imaging together with novel TCO probes, resulting in the selective and rapid labeling of SKOV-3 cells. Our approach may be useful for in vivo pretargeted imaging.

Introduction

Molecular imaging is a powerful tool which enables the non-invasive visualization and quantification of biological processes occurring at cellular level. Recently, the possibility to combine molecular imaging with bioorthogonal chemistry has strongly improved the applicability of this technique for *in vitro* and *in vivo* imaging under different modalities.

Generally, the term "bioorthogonal chemistry" refers to any chemical reaction that can occur inside a living system without interfering with native biochemical processes, and permits the covalent attachment of a probe molecule to a biomolecule of interest. [1–3] In order to achieve bioorthogonal ligation two successive steps are required: (1) introduction of a bioorthogonal tag onto the biological target (pretargeting step), and (2) reaction between the bioorthogonal tag and an externally introduced chemical probe (targeting step).

A well-established bioorthogonal reaction is the Inverse Electron-Demand Diels-Alder (IEDDA) cycloaddition between 1,2,4,5-tetrazines and *trans*-cyclooctene (TCO). This reaction was introduced in 2008 [4–6] and is currently investigated for many applications. [7] In fact, its extremely fast kinetics [8,9] enables application for *in vivo* studies where reactions must occur rapidly at micro- to nanomolar concentrations.

Noteworthy, tetrazine/TCO ligation has been used for pretargeted imaging of tumors both in living cells [10–13] and in mice. [14–16] In a typical bioorthogonal pretargeting approach the target (e.g. cell surface antigen) is first bound by a TCO-modified antibody (Ab), and then a tetrazine probe is provided in order to achieve the labeling through the cycloaddition reaction.

Different TCO-Ab conjugates have been developed in the last years. These conjugates can be obtained either *via* the reaction between TCO-*N*-hydroxysuccinimide (TCO-NHS) esters and the Ab lysine residues, [17,18] or *via* a two-step procedure where the Ab is first decorated with azide functionalities and subsequently reacted with dibenzylcyclooctyne-TCO derivatives (DBCO-TCO). [19] Moreover, the TCO moieties can be attached to the Ab either directly or through short PEG spacers. Even though the type of

[a]Laboratory of Medicinal Chemistry, University of Antwerp, Belgium
[b]Molecular Imaging Center Antwerp, University of Antwerp, Antwerp, Belgium
[c]Biomolecular and Analytical Mass Spectrometry, University of Antwerp, Belgium
[d] Antwerp University Hospital, Department of Nuclear Medicine, Edegem, Belgium
†Correspondence: koen.augustyns@uantwerpen.be

Footnotes relating to the title and/or authors should appear here.
Electronic Supplementary Information (ESI) available: [details of any supplementary information available should be included here]. See DOI: 10.1039/x0xx00000x

View Article Online
DOI: 10.1039/C6OB01411A

attachment does typically not affect the Ab binding affinity, which is usually retained even at high TCO loadings, it can influence the effective number of reactive TCO moieties. Recently, Haun and co-workers have shown that when hydrophobic TCOs are directly attached to the antibody, up to 90% are not reactive due to their tendency to bury within the protein. In contrast, the introduction of TCOs through hydrophilic PEG linkers results in a fully preserved reactivity. [19] Previous to this study, Robillard and co-workers described an *in vivo* deactivation of TCO *via* isomerization to the unreactive *cis*-cyclooctene (CCO). Isomerization is probably catalyzed by copper bound to serum proteins, and its extent depends on the degree of exposure of the TCO tags on the Ab surface. Particularly, it has been demonstrated that the attachment of TCOs through PEG linkers results in a shorter half-life of the tags compared to direct attachment. [18]

Attaining a high Ab functional density is an important feature for the application of bioorthogonal pretargeting in animal models, where a high target-to-background ratio is desirable. The latter may be significantly reduced by both hydrophobic burying and tag exposure deactivation. Due to the slow clearance of intravenously injected Abs, it can take several days to obtain an optimal biodistribution resulting in a prolonged exposure of the TCO tags to physiological environment with consequent deactivation.

Replacement of TCO tags with more hydrophilic tetrazines (inversion of functionalities) could offer a valid alternative to conventional Ab-pretargeting strategies, and may address hydrophobic burying. Moreover, with respect to future in *vivo* applications, the use of more hydrophobic labeled TCOs for targeted imaging might have an advantage to labeled tetrazines when cell membranes or the blood-brain-barrier need to be crossed

To date, the use of tetrazines as bioorthogonal tags for antibody-pretargeting has not been investigated. However, several studies demonstrated the utility of tetrazines as tags for pretargeted protein labeling, [20–23] and construction of labeled peptides. [24–26] Yi and co-workers reported the use of a Ab-tetrazine conjugate for protein capture. [27] Han *et al.* described Ab-quantum dot (QD) conjugates, which were assembled by reacting Ab-tetrazine conjugates with norbornene-coated QDs. [28] A challenge for the use of tetrazine-Ab conjugates for bioorthogonal-pretargeting is the development of tetrazines displaying long term stability under physiological conditions and, at the same time, high reactivity for the IEDDA reaction. Monoaryl-1,2,4,5-tetrazines and 3,6-di-(2-pyridyl)-1,2,4,5-tetrazines, commonly employed as bioorthogonal probes, exhibit fast kinetics but are susceptible to degradation in biological environments. [11,29]

Here we present the synthesis and characterization of a series of tetrazines bearing diverse substituents. We evaluated their stability and reactivity for the IEDDA reaction with (*E*)-cyclooct-4-enol and validated the use of these compounds for antibody labeling. Most importantly, we developed a novel Ab-tetrazine conjugate which displays a good long-term physiological stability, high functional density, and fast kinetics with TCO modified-fluorophores. Furthermore, we demonstrate the effectiveness of the Ab-tetrazine conjugate using pretargeted cancer cell studies as validation platform.

Results and discussion

Chemical Synthesis of 1,2,4,5-Tetrazine Derivatives

The first step towards our goal was the development of a tetrazine derivative exhibiting an optimized compromise in terms of reactivity and stability. To this end we investigated the effect of different substituents on the tetrazine core and developed a total of 8 compounds (Figure 1). Furthermore, all compounds were designed to possess a functional conjugation handle for antibody modification, such as a 5-oxopentanoic or a propionic acid chain.

Compounds **1**-**5** where prepared following a modification of a previously reported procedure which entails the reaction between nitrile and amidine precursors with hydrazine monohydrate in presence of a catalyst (sulfur or zinc triflate), followed by oxidation of the dihydrotetrazine intermediates (Figure 1A). [30] After purification, tetrazines **1-5** were obtained in yields ranging from 11 to 40%. The comparatively moderate yields apparently derive from the use of hydrazine monohydrate, which is more convenient and safe to use, instead of anhydrous hydrazine that was employed in the original procedure. [30]

The synthesis of compounds **6-8** was performed through a two-step protocol, where tetrazines bearing thiomethyl- or 3,5-dimethyl-1-pyrazol-1-yl (DMP) leaving groups were subjected to nucleophilic substitution with 4-aminobenzylamine. The resulting amino-derivatized tetrazine intermediates where subsequently reacted with glutaric anhydride to yield the final products in good overall yields (from 54 to 76% over two steps) (Figure 1B).

Figure 1. Synthesis of tetrazine derivatives and TCO fluorescent dyes

View Article Online
DOI: 10.1039/C6OB01411A

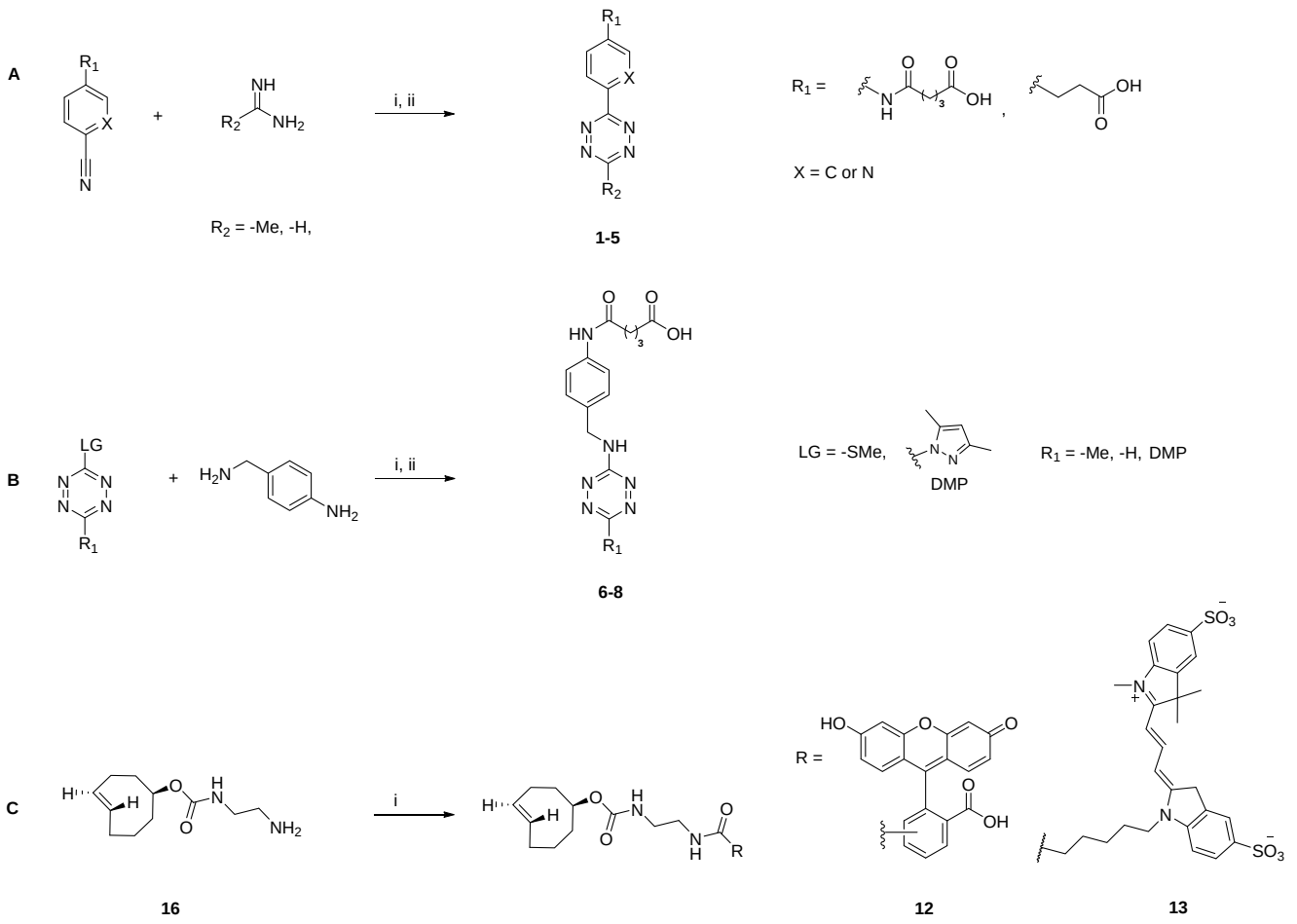

(A) Synthesis of tetrazine **1-5**, reaction conditions: (i) $Zn(OTf)_2$ or S_8, $NH_2NH_2{\cdot}H_2O$, EtOH, r.t.; (ii) $NaNO_2$, HCl 1M, H_2O, 0 °C; (B) Synthesis of tetrazine **6-7**, reaction conditions: (i) MeOH or toluene, r.t., Ar; (ii) glutaric anhydride, THF, reflux; (C) Synthesis of TCO dyes **12** and **13**, reaction conditions: (i) Dye-NHS ester, DMF, TEA, r.t., N_2.

Tetrazine Stability and Reaction Kinetics with (*E*)-cyclooct-4-enol

The stability of the newly synthesized compounds was investigated next. Tetrazines **1**-**8** were incubated in either phosphate buffered-saline (PBS) or pure fetal bovine serum (FBS) at 37 °C, and the decrease of the tetrazine absorbance at selected wavelengths was monitored. The proportion of intact tetrazine was determined after four days (see Table 1). The stability of tetrazines **9** and **10**, which are commonly used for bioorthogonal studies and thus serve as reference control, was also evaluated and compared to that of the newly synthesized compounds. As could be predicted tetrazines containing electron donating groups (compounds **6**-**8**) turned out to be very stable in either PBS or FBS, with up to 100% remaining intact after 4 days. On the other hand, for aryl substituted tetrazines (compounds **1-5**) the stability was considerably reduced by replacing a methyl group with a hydrogen on the tetrazine core, and by the presence of electron withdrawing groups on the aryl substituent. The least stable compounds turned out to be tetrazines **2** and **10** with measured half-lives in PBS of 2 and 9 h respectively (Table 1).

The reactivity of tetrazines **1**-**9** towards the IEDDA reaction with (*E*)-cyclooct-4-enol was also evaluated (Table 1). Since the rate of the reaction between compounds **1**-**5** and the dienophile was too fast for reliable determination *via* UV-vis experiments, the reaction rates were measured by ^{1}H-NMR competition experiments with 3,6-di-2-pyridyl-1,2,4,5-tetrazine (DIPY).

View Article Online
DOI: 10.1039/C6OB01411A

Table 1. Stability data and second order rate constants for tetrazines **1**-**10**

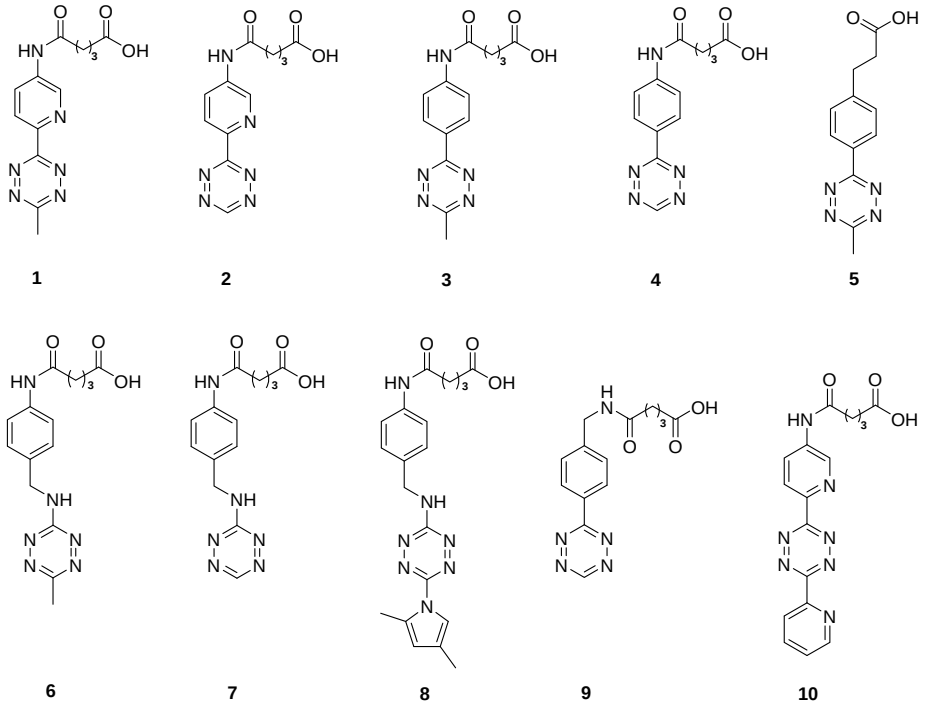

Compound	Stability PBS % Intact at 4 days[a] (t½, h)[b]	Stability FBS % Intact at 4 days[a] (t½, h)[b]	k_2 (M^{-1} s^{-1}) Reaction with (*E*)-cyclooct-4-enol	Reaction Solvent[c]
1	48 ± 1	19 ± 4 (16)	210 ± 42	MeOH
2	0 (2)	-	902 ± 164	MeOH
3	96 ± 1	40 ± 20 (82)	136 ± 54	MeOH
4	41 ± 2	23 ± 15 (26)	875 ± 84	MeOH
5	100 ± 2	84 ± 6	95 ± 15	MeOH
6	100 ± 12	100 ± 6	0.41 ± 0.02	PBS
7	98± 2	95 ± 9	9.3 ± 0.6	PBS
8	89 ± 5	69 ± 30	0.31 ± 0.04	PBS
9	34 ± 1	19 ± 4 (23)	807 ± 145	MeOH
10[d]	0 (9)	-	-	-

(a) Data normalized to 100% at t = 0 h, and reported as mean value of three measurement ± SD; (b) half life in brackets; (c) temperature: 25 °C for reactions performed in MeOH, 37 °C for reactions performed in PBS; (d) the k_2 of tetrazine **10** could not be determined due to its poor solubility in MeOH.

View Article Online
DOI: 10.1039/C6OB01411A

In fact, the second order rate constant (k_2) of DIPY for the reaction with (*E*)-cyclooct-4-enol in MeOH is known to be 820 M^{-1} s^{-1}. [9] After mixing DIPY, the dienophile and the selected tetrazine in MeOH the ^{1}H NMR of the mixture was analyzed, and the conversion rates of the two tetrazines determined. From the relative conversion rates the final rate constants were calculated.[31]

Due to their slower kinetics, the cycloaddition rates of tetrazines **6**-**8** could be directly measured by UV-Vis experiments. The rate constants were determined in PBS at 37°C by reacting the different compounds with the dienophile under pseudo first order conditions, and measuring the disappearance of the tetrazine adsorption at selected wavelengths.

From this study we determined that the reactivity of aryl tetrazine **1**-**5** is inverse to their stability. Whereas, for compounds **6**-**8** the presence of a hydrogen substituent on the tetrazine ring strongly affects the reactivity, with tetrazine **7** being 20 to 30 fold more reactive than tetrazines **6** and **8**.

Overall, the range of reactivities and stabilities covered by compounds **1**-**8** make this library a valuable addition to the tetrazine compounds currently available for bioorthogonal pretargeting.

From these screenings we conditionally selected tetrazine **3** for the biological studies. This compound showed the best profile with regard to stability and reactivity with a half-life of 82 h in serum at 37 °C , and a k_2 of 136 M^{-1} s^{-1} in MeOH at 25 °C (Table 1). Noteworthy, the *in vitro* stability of tetrazine **3** is substantially higher compared to that of TCO derivatives commonly used for Ab modification, for which half-lives of circa 3 h were reported in serum. [18] The low rate constant of compound **3** in MeOH may rise in aqueous media. In fact, it has been previously demonstrated that the rate of the IEDDA reaction is accelerated by increasing solvent polarity and temperature. [32] This observation has been confirmed for tetrazine **9**, which possesses a k_2 of 6000 M^{-1} s^{-1} as has been reported under physiological conditions. [10] For antibody modification tetrazine **3** was converted to the corresponding *N*-hydroxysuccinimide (NHS) ester derivative, tetrazine-NHS **11**.

Development and Characterization of the Antibody-Tetrazine Conjugate

The next step in our study was the development of an Ab-tetrazine conjugate where tetrazine **3** is used as bioorthogonal tag. To this end, anti-HER2/neu antibody trastuzumab was selected as the model antibody and tagged with tetrazine **3** *via* standard amine-coupling procedure.

The tetrazine loading was modulated using two different molar equivalents (10 and 100) of the amino reactive tetrazine, and the number of incorporated tags was determined by quadrupole-time-of-flight (Q-TOF) mass spectrometry. To this end, trastuzumab was used as reference and its mass spectrum compared to that of the trastuzumab-tetrazine **3** conjugates. As shown in Figure 3A the mass spectrum of trastuzumab reveals the presence of a 148 117 Dalton (Da) Ab with charge states from 22+ to 27+. For comparison we selected the most intense peak (25+ charge state), and determined that treatment of trastuzumab with 10 equivalents of the tetrazine-NHS **11** resulted in the incorporation, on average, of 2 tetrazine tags per antibody. Whereas, an average of 8 tags was incorporated after treatment with 100 equivalents (Figure 3B).

Figure 3. Mass spectra of the trastuzumab-tetrazine **3** conjugates

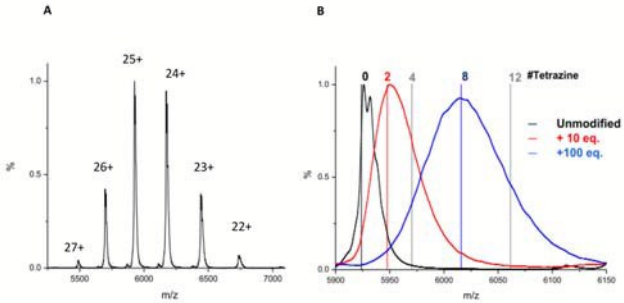

(A) Mass spectrum of trastuzumab (148117 Da) with charge states from 22^+ to 27^+; (B) 25^+ charge state of trastuzumab (black) compared to trastuzumab-tetrazine **3** conjugates after treatment with 10 (red) and 100 (blue) equivalents of tetrazine-NHS **11**.

The number of reactive tetrazines per antibody was also evaluated based on absorbance readings after reaction with an excess of TCO-fluorescein dye (**12**). We observed that there are 0.4 and 5 reactive tetrazines for the conjugate bearing 2 and 8 tags, respectively. Remarkably, 62% of tetrazine moieties resulted active for the conjugate bearing 8 tags. This result indicates that the direct attachment of tetrazine tags on the antibody does not influence their reactivity, with high number of tags remaining functional towards the cycloaddition reaction.

The reaction rate of the trastuzumab-tetrazine **3** conjugate with TCO-fluorescein dye (**12**) was determined next. To this end, the

View Article Online
DOI: 10.1039/C6OB01411A

immunoconjugate was reacted with different excess of **12** in PBS at 37 °C. At selected time points aliquots were taken, and the reaction was quenched by addition of (*E*)-cyclooct-4-enol to the mixtures. After removal of the unreacted dienophiles the fluorescence signal was monitored over time and pseudo-first-order rate constants (k_{obs}) were obtained (Figure S6). From the different k_{obs} a k_2 of 3083 ± 352 M^{-1} s^{-1} was determined. As anticipated, the resulting rate constant was higher than that measured for tetrazine **3** in MeOH (k_2 = 136 M^{-1} s^{-1}).

Binding affinity of the trastuzumab-tetrazine 3 conjugate for HER2/neu receptors

We set out to determine whether the binding affinity of the immunoconjugate for the receptors is retained, and performed a saturation binding assay where triple negative human breast adenocarcinoma (MDA-MB-231, Her-2/neu negative) and human ovarian adenocarcinoma (SKOV-3, Her-2/neu positive) cells were used as negative and positive control respectively. Before proceeding with the assay, cell lines were subjected to short tandem repeats (STR) and fluorescent in situ hybridization (FISH) analysis. The STR loci were concordant with the information given by the manufacturer (ATCC Rockville, Maryland) and in all tumor cell lines the hybridization signal was uniform. Whereas, FISH analysis demonstrated high ratio HER-2/neu over chromosome 17 in SKOV-3 (3.16), but no detectable expression in MDA-MB-231 cells.

Figure 4. Saturation plot

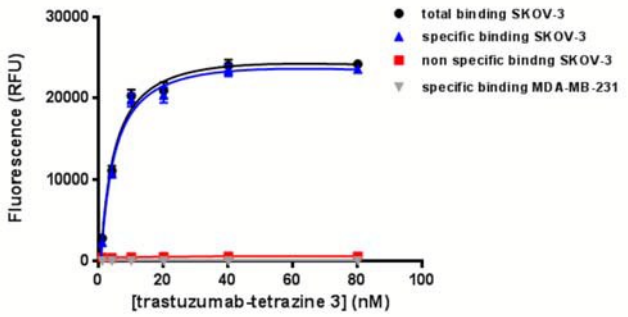

Binding of the trastuzumab-tetrazine-**3**-TCO-fluorescein conjugate to SKOV-3 and MDA-MB-231 cells. Specific binding was defined as total binding minus non-specific binding obtained by incubation of the immunoconjugate with 1µM trastuzumab.

In imaging studies, a high Ab functional loading is desirable therefore we selected for the binding assay the trastuzumab-tetrazine **3** conjugate with the highest tetrazine loading (8 tags per Ab). In order to introduce a fluorescent label and enable the tracking of the antibody on the cells, the immunoconjugate was reacted with TCO-fluorescein dye **12**.

After incubation of the cells with this "pre-clicked" trastuzumab-tetrazine-**3**-TCO-fluorescein conjugate we determined a dissociation constant (K_D) of 3.9 nM which correlates with that of native trastuzumab (K_D = 5 nM as reported by the manufacturer), and that there is no unspecific binding to the cells (Figure 4).

This result demonstrates that the binding affinity of the immunoconjugate is retained even with the higher tetrazine loading, and that this conjugate is suitable for cell imaging experiments.

Cell imaging experiments

To obtain a prove of concept for our approach we performed pretargeted cell imaging experiments using the newly developed trastuzumab-tetrazine **3** conjugate in combination with TCO fluorescent probes (Figures 5 and 6).

Figure 5. Pretargeting Scheme

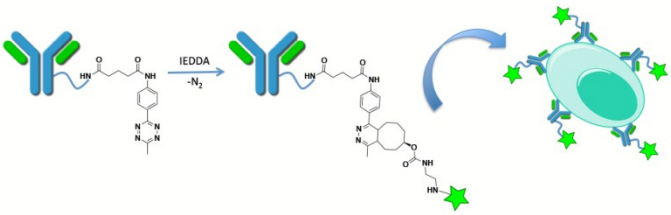

Cells are pretargeted with trastuzumab-tetrazine **3** conjugates, and labeled with TCO fluorescent dyes *via* the IEDDA cycloaddition.

To this end, SKOV-3 cells were incubated with 50 nM of the immunocojugate bearing 8 tetrazine tags. After washing, Ab labelled cells were treated with two different concentrations of TCO dye **12** (0.5 and 10 µM), washed again, and then imaged in the green fluorescent probe (GFP) channel. As shown in figure 6A, considerable membrane labelling was obtained for cells treated with trastuzumab-tetrazine **3** even at low dye concentration.

View Article Online
DOI: 10.1039/C6OB01411A

Figure 6. Fluorescent microscopy images

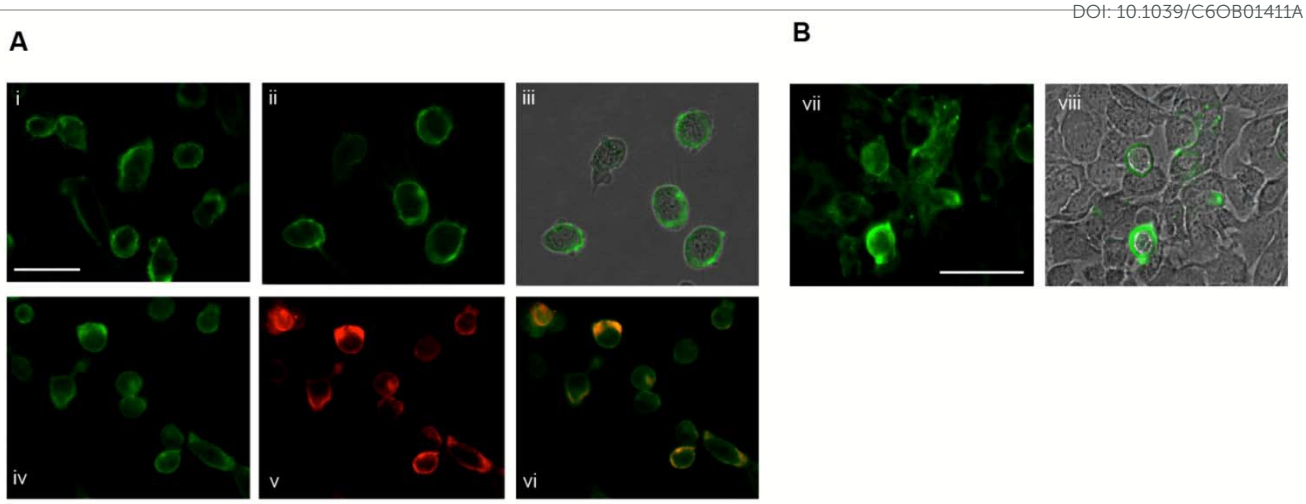

(**A**) Images of SKOV-3 cells treated with trastuzumab-tetrazine **3** conjugates for 45 min. (i-iii) Cells were treated with trastuzumab-tetrazine **3** 0.05 µM: (i) after treatment with dye **12** 0.5 µM, (GFP channel), (ii) after treatment with dye **12** 10 µM (GFP channel), (iii) example of overlay of GFP channel and differential interference contrast (DIC). (iv-vi) Cells were treated with trastuzumab-tetrazine **3** fluorescein 0,5 µM: (iv) image in the GFP channel, (v) after treatment with dye **13** 10 µM (RFP channel), (vi) merged image of iv and v. (**B**) Images of SKOV-3 cells treated with trastuzumab-tetrazine **3** conjugate 0,05 µM for 48 h: (vii) after treatment with dye **12** 10 µM (GFP channel), (viii) overlay of GFP and DIC. Positive and negative controls in supporting information (FigureS7). Scale bar: 50 µm.

To track the antibody on the cells and at the same time verify the specificity of the bioorthogonal reaction, a dual labeled Ab-conjugate was also utilized.

The latter was prepared by treating trastuzumab with both tetrazine-NHS **11** and fluorescein-NHS ester. In this case, the Ab labeled cells where treated with Cy3 dye **13**, and imaged using both GFP and red fluorescent probe (RFP) channels. The labeling of the cells was observed on both channels with good colocalization of the signal (Figue 6A iv-vi).

Negative controls were obtained by incubation of SKOV-3 cells with dyes **12** and **13**, showing no unspecific labeling (Figure –S7 iii-iv). Cells were also labeled with control antibodies trastuzumab-fluorescein and the "pre-clicked" trastuzumab-tetrazine-**3**-TCO-fluorescein (Figure S7i-ii).

With the perspective of applying our Ab-tetrazine conjugate for *in vivo* studies we decided to assess its stability towards prolonged exposure to biological media. Particularly, we evaluated the stability of the trastuzumab-tetrazine **3** conjugate under cell labelling conditions by extending the Ab incubation time from 45 minutes to 48 hours. Membranous staining of the cells could still be observed after treatment with dye **12**, indicating that the tetrazine moieties are still reactive (Figure 6B).

These experiments clearly demonstrate the effectiveness of our Ab-tetrazine conjugates as pretargeting agents for bioorthogonal imaging in an *in vitro* set-up

Conclusions

Due to their high target specificity, yet long circulation times within the body, Abs represent an excellent platform for bioorthogonal pretargeting both in cell and animal models. In fact, bioorthogonal pretargeting can significantly improve the target-to-background ratio resulting in a better target visualization and quantification compared to conventional immunotargeting techniques.

Since the introduction of the tetrazine/TCO ligation, many studies have reported the use of TCO modified Abs for pretargeted tumor imaging. However, the inverse approach has not been investigated yet, although inverting the TCO with the tetrazine may address some issues related to the use of Ab-TCO conjugates. Particularly, the higher hydrophilicity of tetrazine compounds may

View Article Online
DOI: 10.1039/C6OB01411A

prevent hydrophobic burying of the tags within the protein resulting in a higher effective functional loading.

In this study we developed a novel Ab-tetrazine conjugate and obtain a proof of concept for its applicability using real-time fluorescence cell imaging as validation method. We synthesized a small library of novel 1,2,4,5-tetrazines all suitable for protein modification, and selected compound **3** for antibody labeling. This tetrazine displays a remarkable stability towards physiological media and still retains a good cycloaddition reactivity with the TCO. Next, we developed a novel antibody-tetrazine conjugate using tetrazine **3** as bioorthogonal tag. The novel immunoconjugate was evaluated for pretargeted live cell imaging using two different TCO fluorescent probes as imaging agents. This study demonstrates the viability of our approach, showing that the reaction between the Ab-tetrazine construct and TCO probes is fast even at micromolar concentrations and, that the tetrazine tags are unaffected by prolonged exposure to physiological conditions. The high reactivity combined with the good functional density and stability of the Ab-tetrazine conjugate, suggest that this strategy may be useful for *in vivo* positron emission tomography (PET) imaging. This will allow the *in vivo* translation of this approach.

Experimental

General procedures for the synthesis of 1,2,4,5-tetrazines

Method A (compounds **1**-**5**): Compounds **1-5** were synthesized by suspending 5-((4-cyanophenyl)amino)-5-oxopentenoic acid (**14**), 5-((6-cyano)-3-pyridinyl)-5-oxopentenoic acid (**15**) or 3-(4-cyanophenyl)-propanoic acid (1 eq) in EtOH (2 mL). Acetamidine hydrochloride or formamidine acetate (4 to 10 eq) was added followed by sulfur (1 eq) or zinc triflate ($Zn(OTf)_2$, 0.5 eq) and hydrazine hydrate (1.8 mL). The mixture was stirred at room temperature under argon for 16 to 48 h. Then it was diluted with water and cooled to 0°C. $NaNO_2$ (10 eq) was added, followed by dropwise addition of 1M HCl. The acid was added until reaching pH 3. At this point gas evolution started and the solution turned pink or fuchsia (**Caution**! This step generates a large amount of toxic nitrogen oxide gas). The mixture was stirred at 0°C until gas evolution ceased, then EtOAc was added and the organic phase separated. The aqueous phase was extracted three times with EtOAc. The combined organic phases were washed once with brine, and dried over $MgSO_4$. After removal of the solvent the crude residue was adsorbed onto celite and subjected to reverse phase column chromatography (H_2O:MeOH gradient 95:5 to 20:80).

Method B (compounds **6**-**8**)**:** Compounds **6**-**8** were synthesized by dissolving 3,6-bis-(DMP)-1,2,4,5-tetrazine (1 eq), 3-methyl-6-thiomethyl-1,2,4,5-tetrazine (1 eq) [33] or 6-thiomethyl-1,2,4,5-tetrazine (1 eq) [33] in toluene (dry, 1 mL) or methanol (dry, 2 mL). 4-Aminobenzylamine (1 eq) was added to the solution and the mixture was stirred at room temperature for 2 to 4 h under argon. After evaporation of the solvent the crude residue was adsorbed onto silica and subjected to column chromatography. The obtained amino derivatized tetrazines were subsequently refluxed with glutaric anhydride (5 eq) in THF (dry, 2 mL) for 16 h. The final products were purified by reverse phase column chromatography (H_2O:MeOH, gradient 95:5 to 0:100).

General procedure for the synthesis of TCO dyes 12 and 13

(*E*)-cyclooct-4-en-1-yl-(2-aminoethyl) carbamate (**16**) (1 eq.) was dissolved in anhydrous DMF (1mL). Triethylamine (2 eq.) was added, followed by dye-NHS derivatives (1.5 eq.). The mixture was stirred overnight at room temperature under N_2. After evaporation of the solvent, the crude residue was purified by HPLC on a C-18 column (H_2O:ACN isocratic 70 : 30 + 0.1% FA) and freeze-dried. The ^{1}H-NMR spectrum of compound **13** (Figure S3) revealed the presence of a 1 : 1 mixture of *trans* and *cis* isomers. Due to the very low reactivity of the *cis* isomer towards the iEDDA reaction the mixture was used as such for the cell imaging experiments. For simplicity we refer only to the *trans* isomer in figure 1.

Antibody Labeling

Trastuzumab (Herceptin®, Roche) stock in PBS pH 7.4, 144 µM (21 mg/mL) was diluted to a final concentration of 6.9 µM by addition of a PBS solution buffered at pH 9.1. The NHS ester derivative of tetrazine **3** (tetrazine-NHS **11**) was dissolved in DMSO to make a 60 mM stock solution. For conjugation the appropriate excess of tetrazine was aliquoted into the antibody solution, vortexed and reacted for 3 hours at 37 °C. The excess of tetrazine used in this experiment were 10 and 100 equivalents with respect to the antibody. The resulting Ab conjugates were purified via size exclusion chromatography (PD-10 column 5K MWCO, GE Healthcare), concentrated to 1 mg/mL and stored in PBS at 4 °C. A dual labeled trastuzumab conjugate was obtained following a similar procedure where trastuzumab was simultaneously

View Article Online
DOI: 10.1039/C6OB01411A

incubated with 100 equivalents of tetrazine-NHS **11**, and 15 equivalents of fluorescein-NHS ester.

Native mass spectrometry

The mass spectrometry experiments were performed on a Q-TOF-2TM instrument (Micromass, Waters). The samples were buffer exchanged twice into 150 mM aqueous ammonium acetate at pH 7.0 using Micro Bio-Spin P-6 columns (Bio-Rad) at concentrations of 10 µM. Gold-coated nanoESI needles were prepared in-house in order to transfer 5 µL aliquots of sample into the mass spectrometer. The instrument was tuned using the following parameters: capillary voltage 1.6 kV; nanoflow backing pressure 0.3 bar; sample cone 200 V; extractor 10 V ; collision energy 100 V; backing pressure 4.0 mbar. The data were acquired and processed with Masslynx v4.1 software (Waters).

Measurement of Tetrazine Reactive Tags on Antibody

Trastuzumab-tetrazine **3** conjugates (18 µM) were treated with 20 fold excess of TCO-fluorescein dye **12** with respect to the Ab. The reaction was performed in PBS containing 1% of DMSO. After incubation for 1h at 37 °C, the antibody conjugates were purified *via* size exclusion chromatography (PD-10 column 5K MWCO, GE Healthcare), and subjected to UV-vis analysis using the following molar extinction coefficients: $\boldsymbol{\varepsilon_{280}}$ = 225.000 cm^{-1} M^{-1} for trastuzumab, [34] and $\boldsymbol{\varepsilon_{500}}$ = 70.000 cm^{-1} M^{-1}, CF = 0.3 (Thermo Scientific) for dye **12**. Unmodified Trastuzumab was subjected to the same treatment and used as reference for these experiments. Each experiment was repeated in triplicate. Fluorescent spectra of the Ab conjugates were also recorded after treatment with dye **12** (FigureS5).

Cell culture

Her-2/neu negative MDA-MB-231 and Her-2/neu overexpressing SKOV-3 cell lines were purchased from ATCC (Rockville, Maryland). Cells were routinely cultured in Dulbecco's Modified Eagle Medium (DMEM) and DMEM/F12 medium respectively, supplemented with 10% (or 5% for SKOV-3 cells) heath inactivated FBS, 2 mM glutamine, 1% sodium pyruvate and 1% penicillin/streptomycin (Gibco, Life technologies). Cultures were maintained in exponential growth at 37°C in a humidified atmosphere containing 5% CO_2. The HER-2 status was evaluated by FISH analysis. The identity of cell lines was confirmed with STR profiling. An 80-90% confluent culture was detached with trypsin-EDTA or accutase (for SKOV-3) and washed three times with 1 x PBS to remove any cell debris. Cells were counted with the Muse System (Merck Millipore, Count and Viability Assay kit) and resuspended in their respective medium in a concentration of 1 x 10^6 viable cells/0.5 ml.

Cell saturation binding assay

Trastuzumab-tetrazine **3** conjugate with the highest tetrazine loading (8 tags per antibody) was reacted with dye **12** (7.4 eq. with respect to the antibody). After purification (PD-10 column 5K MWCO, GE Healthcare), the resulting fluorescent conjugate, bearing 4 fluorophore moieties, was utilized for the saturation binding assay.

Briefly, increasing concentrations of the antibody conjugate (1 nM -80 nM, quadruplicate) were incubated with 1 x 10^6 SKOV-3 or MDA-MB-231 cells in a total volume of 1 mL cell medium for 2 h at 4°C. To assess non-specific binding, unmodified trastuzumab (1µM) was added (duplicates). Following incubation, the cells were pelleted *via* centrifugation (2000 rpm for 5min at 4°C) and, after removal of the supernatant, washed with cold 1 x PBS + 0.2% tween 20 solution (repeated twice). After the last washing step the cells were resuspended in 500 µL 1 x PBS and 200 µL aliquots from each tube were transferred to a 96-well plate (Nunclon Delta Surface, Thermo scientific) and the fluorescence intensity of the samples was measured (λ_{ex} = 500 nm, λ_{em} = 550 nm). The fluorescence intensity with Ab concentration was fitted to a first-order exponential using GraphPad Prism 6, and the K_D determined to be 3.9 nM.

Cell microscopy

Trastuzumab-tetrazine **3** (0.05 µM), and trastuzumab-tetrazine-**3**-fluorescein (0.5 µM) were incubated with 150.000 cells plated into 6-well plates, for 45 min in DMEM/F12 without phenol red, containing 5% FBS, 2 mM glutamine, 1% sodium pyruvate and 1% penicillin/streptomycin. Cells were then washed 3x with cell medium before incubating with 0.5 and 10 µM of dyes **12** and **13** for 30 min in growth media. After washing 3 times with sterile 1 x PBS, images were taken using an EVOS fluorescence digital inverted microscope in the GFP and RFP channels. Identical image acquisition settings were used for the experimental data. Images

View Article Online
DOI: 10.1039/C6OB01411A

were analyzed using ImageJ applying identical leveling adjustments to all experimental data across individual channels.

ACKNOWLEDGMENTS

We thank Prof. Yves Guisez for his support on the mass analysis of the immunoconjugates; and Prof. Filip Lardon for access to the microscope. This work was supported by grants from the University of Antwerp (GOA-BOF) and FWO-IWT.

REFERENCES

1 R. K. V Lim, Q. Lin, *Chem. Commun.*, 2010, ***46***, 1589.

2 C. S. McKay, M. G. Finn, *Chem. Biol.* 2014, ***21***, 1075.

3 E. M. Sletten, C. R. Bertozzi, *Angew. Chem. Int. Ed.*, 2009, ***48***, 6974.

4 M. L. Blackman, M. Royzen, J. M. Fox, *J. Am. Chem. Soc.*, 2008, ***130***, 13518.

5 N. K. Devaraj, R. Weissleder, S. A. Hilderbrand, *Bioconjugate Chem.*, 2008, ***19***, 2297.

6 K. Braun, M.Wiessler, V. Ehemann, R. Pipkorn, H. Spring, J. Debus, B. Didinger, M. Koch, G. Muller, W. Waldeck, *Drug. Des. Devel .Ther.*, 2008, **2**, 289.

7 H. Wu, N. K. Devaraj, *Top. Curr. Chem.*, 2015, *374:3*.

8 A. Darko, S. Wallace, O. Dimitrenko, M. M. Machovina, R. A. Mehl, J. W. Chin, J. M. Fox, *Chem. Sci.*, 2014, ***5***, 3770.

9 M. T. Taylor, M. L. Blackman, O. Dmitrenko, J. M. Fox, *J. Am. Chem. Soc.*, 2011, ***28***, 9646.

10 N. K. Devaraj, R. Upadhyay, J. B. Haun, S. A. Hilderbrand, R. Weissleder, *Angew. Chem*, 2009, ***48***, 7013.

11 M. R. Karver, R. Weissleder, S. A. Hilderbrand, *Bioconjugate Chem.*, 2011, ***22***, 2263.

12 L. G. Meimetis, J. C. T. Carlson, R. J. Giedt, R. H. Kohler, R. Weissleder, *Angew. Chem. Int. Ed*, 2014, 7531.

13 I. Nikič, T. Plass, O. Schraidt, J. Szymański, J. A G. Briggs, C. Schultz, E. A. Lemke, *Angew. Chem. Int. Ed*, 2014, ***53***, 2245.

14 R. Rossin, M. S. Robillard, *Curr. Opin. Chem. Biol*, 2014, ***21***, 161.

15 B. M. Zeglis, C. Brand, D.Abdel-Atti, K. E. Carnazza, B. E. Cook, S. Carlin, T. Reiner, J. S. Lewis, *Mol. Pharm.*, 2015, ***12***, 3575.

16 J. P. Meyer, J. L. Houghton, P. Kozlowski, D. Abdel-Atti, T.Reiner, N. V. K. Pillarsetty., W. W.Scholz, B. M. Zeglis, J. S. Lewis, *Bioconjugate Chem.*, 2016, ***27***, 298.

17 J. B. Haun, N. K. Devaraj, S. A Hilderbrand, H. Lee, R. Weissleder, *Nat. Nanotechnol.*, 2010, ***5***, 660.

18 R. Rossin, S. M. van den Bosch, W. Ten Hoeve, M. Carvelli, R. M. Versteegen, J. Lub, M. S. Robillard, *Bioconjugate Chem.*, 2013, ***24***, 1210.

19 M. K. Rahim, R. Kota, J. B. Haun, *Bioconjugate Chem.*, 2015, ***26***, 352.

20 R. J. Blizzard, D. R. Backus, W. Brown, C. G. Bazewicz, Y. Li, R. A. Mehl, *J. Am. Chem. Soc.*, 2015, ***137***, 10044.

21 H. E. Murrey, J. C. Judkins, C. W. Am Ende, T. E. Ballard, Y. Fang, K. Riccardi, L. Di, E. R. Guilmette, J. W. Schwartz, J. M. Fox, D. S. Johnson, *J. Am. Chem. Soc.*, 2015, ***137***, 11461.

22 J. L. Seitchik, J. C. Peeler, M. T. Taylor, M. L. Blackman, T. W. Rhoads, R. B. Cooley, C. Refakis, J. M. Fox, R. A. Mehl, *J. Am. Chem. Soc.*, 2012, ***134***, 2898.

23 D. S. Liu, L. D. S. Tangpeerachaikul, R. Anupong Selvaraj, M. T. Taylor, J. M. Fox, A. Y. Ting, *J. Am. Chem. Soc.*, 2012, ***134***, 792.

24 Liu, S.; Hassink, M.; Selvaraj, R.; Yap, L.; Park, R.; Wang, H.; Chen, X.; Fox, J. M.; Li, Z.; Conti, P. S. *Mol. Imaging* **2013**, *12*, 121.

25 R. Selvaraj, B. C. Giglio, S. Liu, H. Wang, M. Wang, H. Yuan, S. R. Chintala, L. Yap, P. S. Conti, J. M. Fox, Z. Li, *Bioconjugate Chem.*, 2015, ***26***, 435.

26 Z. Wu, S. Liu, M. Hassink, I. Nair, R. Park, L. Li, I. Todorov, J. M. Fox, Z. Li, J. E. Shively, P. S. Conti, F. Kandeel, *J. N. Med.*, 2013, ***54***, 244.

27 S. Jung, H. Yi, *Langmuir*, 2014, ***30***, 7762.

28 H. S. Han, E. Niemeyer, Y. Huang, W. S. Kamoun, J. D. Martin, J. Bhaumik, Y. Chen, S. Roberge, J. Cui, M. R. Martin, D. Fukumura, R. K. Jain, M. G. Bawendi, D. G. Duda, *Proc. Natl. Acad. Sci.*, 2015, ***112***, 1350.

29 R. Rossin, P. R. Verkerk, S. M. van den Bosch, R. C. M. Vulders, I. Verel, J. Lub, M. S. Robillard, *Angew. Chem. Int. Ed.*, 2010, ***49***, 3375.

30 J. Yang, M. R. Karver, W. Li, S. Sahu, N. K. Devaraj, *Angew. Chem. Int. Ed*, 2012, ***51***, 5222.

31 K. Ingold, R. Shaw, *J. Chem. Soc,*. 1927, 2918.

32 J. W. Wijnen, S. Zavarise, J. B. F. N. Engberts, M. Charton, *J. Org. Chem*, 1996, ***61***, 2001.

33 S. C. Fields, M. H. Parke, E. W. Randal, *J. Org. Chem*, 1994, ***59***, 8284.

34 A. Maeda, J. Bu, J. Chen, G. Zheng, R. S. DaCosta, *Mol. Imaging*, 2014, ***13***, 1.